

# Analysis of Static Friction Coefficient Between Work-piece and Rubber Belt in Sanding Wood-Based Panel

Bin Luo, Li Li,\* Meijun Xu, Hongguang Liu, and Fangru Xing

This study analyzes the critical static friction coefficient ( $\mu_0$ ) and the static friction coefficient ( $\mu$ ) between work-piece and rubber belt during sanding medium density fiberboard (MDF) and particle board (PB). The purpose is to provide theoretical support for improving design techniques of sanding machine and choosing appropriate rubber belts for sanding. The results indicate that  $\mu_0$  is a constant that can be calculated by maximum sanding force ( $sF_{Max}$ ) and maximum normal force ( $nF_{Max}$ ). Besides, there is an exponential relationship between intensity of pressure ( $P$ ) and  $\mu$  when work-piece is relatively static on a rubber belt. Among all sanding parameters, grit size ( $G$ ) has the greatest influence on  $\mu$ . In single-factor experiment, we found that the smaller the  $nF_{Max}$  is, the greater the  $\mu$  is (for same rubber belts), but the variation rates of  $\mu$  and  $nF_{Max}$  are coincident. Six types of rubber belts are adopted, and the average  $\mu$  of No. 1 and No. 4 are greater than others, but average  $\mu$  of all the belts are lower than  $\mu_0$ , so when use such six types of rubber belts, a hold-down device or vacuum chuck should be equipped on the sanding machine. Patterns of rubber belts have some impact on  $\mu$ , and appropriate patterns on the surface of rubber belts contribute to higher  $\mu$ .

*Keywords:* Critical static friction coefficient; Grit size; Medium density fiberboard; Normal force; Particle board; Static friction coefficient; Sanding force

*Contact information:* College of Materials Science and Technology, Beijing Forestry University, No.35 Tsinghua East Rd, Haidian District, Beijing, 100083, P. R. China;

\* Corresponding author: [bjfu\\_lili@126.com](mailto:bjfu_lili@126.com)

## INTRODUCTION

The feed orientation is opposite to the sanding orientation in a sanding process. In the process of feeding, the sanding force ( $sF$ ) is the resistance, and the friction ( $f$ ) between rubber belt and work-piece is the tractive force. The  $f$  should be greater than the  $sF$ ; otherwise, the work-piece will be kicked back. The normal force ( $nF$ ) on the work-piece should be great enough for the normal feed. Meanwhile, the value of  $sF$  also increases with increasing  $nF$ . The method to keep the work-piece relatively stationary on track is increasing the static friction coefficient ( $\mu$ ) between the rubber belt and work-piece (Li and Meng 2000).

The value of  $f$  between the rubber belt and wood based panel (viscous-elastic material) depends on two parts: adhesion and hysteresis (results of the elasticity of both materials). Usually, adhesion is the primary part when a rubber belt slides on the material with smooth surface. But for the material with rough surface, the distortional units of rubber belt would fill into the gaps of the surface, and then the proportion of hysteresis increases (Jun 2008).

In the previous studies, Guan *et al.* (1983) found that the friction coefficient between steel and some Swedish wood species was higher on rougher steel surfaces. For

an isotropic steel, a rougher surface resulted in lower  $f$  under low-speed condition, but under high-speed condition, the situation is the reverse (Masuko *et al.* 2005). The friction coefficient for helical gears increased with the improved surface roughness (Han *et al.* 2013). This study focused on analyzing the critical static friction coefficient ( $\mu_0$ ) and  $\mu$  between work-piece and rubber belt during sanding medium density fiberboard (*MDF*) and particle board (*PB*). The purposes of this study are to provide theoretical support for improving design technics of sanding machine and choosing appropriate rubber belts for sanding.

## EXPERIMENTAL

### Materials

*MDF* and *PB* used in the work had an average density and surface hardness of 0.74 g/cm<sup>3</sup> and 0.99 g/cm<sup>3</sup>, and 51.7 HD and 64.1 HD, respectively. The sizes of work-pieces were 150 x 100 mm (superficial area=0.0015 m<sup>2</sup>) and 63 x 63 mm (superficial area=0.003969 m<sup>2</sup>). Abrasive belts were made by Tianjin Deerfos Co., LTD (base material: twill, grit: white fused alumina, electro coated abrasive and adhesive: phenol formaldehyde resin). Figure 1 shows the characteristics of six rubber belts (HDSY Co., LTD, Shanghai, China), and the surface hardness of them was 19.2 HD.

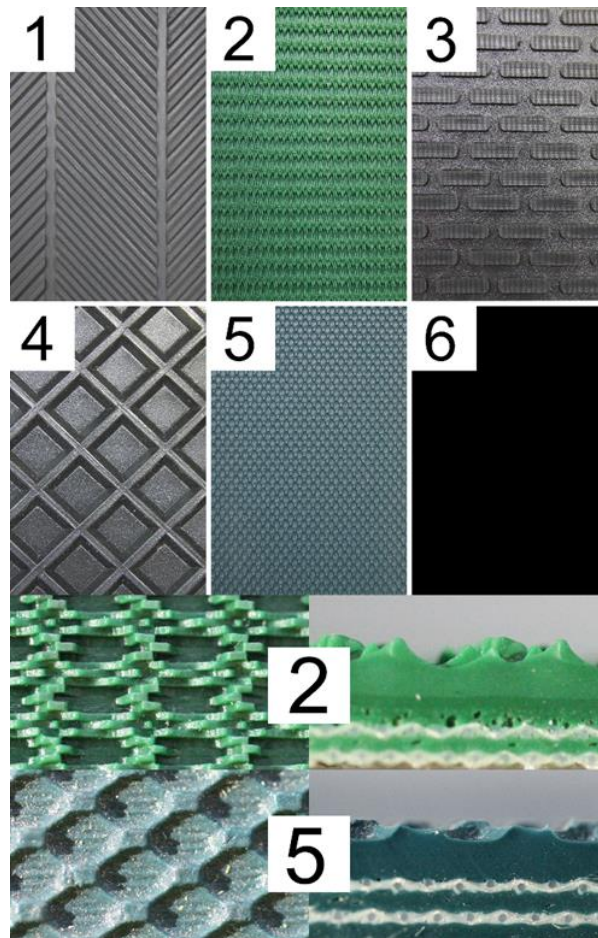


Fig. 1. Rubber belts

The measuring equipment included a 3D force sensor (KISTLER-3257A, Kistler Instrument AG, Winterthur, Switzerland), a charge-amplifier (KISTLER 5806, Kistler Instrument AG, Winterthur, Switzerland), a signal analyzer (NEC Omniace II RA2300, NEC Corporation, Tokyo, Japan), a data acquisition card (USB-7660, ZCTQ co., LTD, Beijing, China), a tension sensor (MCL-S0, ZK Instruments co., LTD, Beijing, China), and a Shore durometer (TH210, THco., LTD, Beijing, China).

## Methods

### Calculating method of relationship between intensity of pressure ( $P$ ) and $\mu$

The testing system in Fig. 2 was used to obtain the relationship between  $P$  and  $\mu$ . The work-piece was connected to the force sensor rigidly. The slide-stroke is 0.12 m, the sliding speed is 0.008 m/s, and the data acquisition frequency is 50 Hz. The  $f$  (equals to maximal tensile force) between work-piece and rubber belt will generate before the work-piece moves, then  $\mu$  is calculated by  $f$  and  $nF$  (equals to counter weight), and  $P$  is calculated by  $nF$  and contact area, as shown in Eqs. 1 and 2. Five counter weights (10, 50, 100, 150, and 200 N) were adopted, with a contact area of 0.003969 m<sup>2</sup> (63 mm x 63 mm). Finally, the relationships between  $P$  and  $\mu$  for six types of rubber belt were obtained by fitting equations.

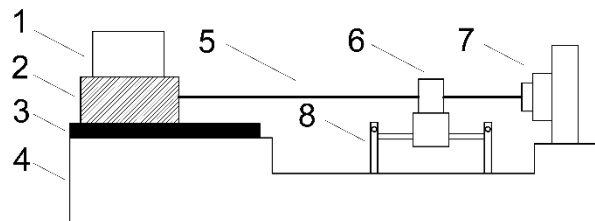


**Fig. 2.** Testing system of obtaining the relationship between  $P$  and  $\mu$  ( $P$ : intensity of pressure,  $\mu$ : static friction coefficient, 1: counter weight, 2: work-piece, 3: rubber belt, 4: pedestal, 5: iron wire, 6: tension sensor (MCL-S0, ZK Instruments co., LTD, Beijing, China), 7: motor, 8: sliding track)

$$\mu = f/nF \quad (1)$$

$$P = nF/\text{contact area} \quad (2)$$

### Calculating method of critical static friction coefficient ( $\mu_0$ )

As shown in Fig. 3, when the work-piece was just relatively stationary on the rubber belt, the resultant force in the horizontal direction is zero. This situation is the critical state, in which the static friction coefficient is called critical static friction coefficient ( $\mu_0$ ).

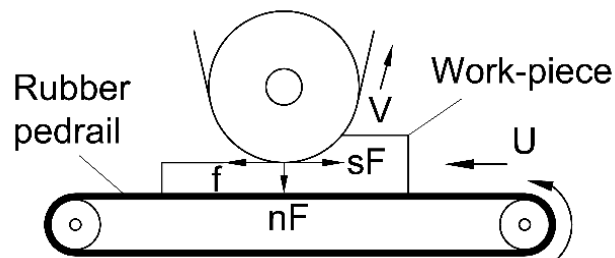


**Fig. 3.** Analysis of critical state of work-piece in sanding process ( $sF_{Max}$ : maximum sanding force,  $nF_{Max}$ : maximum normal force,  $f$ : friction,  $U$ : feed speed,  $V$ : sanding speed)

According to Eq. 3,  $\mu_0$  is calculated by  $sF_{Max}$  and  $nF_{Max}$ . A work-piece will be kicked back if  $f$  is less than maximal sanding force ( $sF_{Max}$ ). In other words,  $\mu$  must be equal to or greater than  $\mu_0$  for normal feed (Eq. 4).

$$f = sF_{Max} = nF_{Max}\mu_0 \quad (3)$$

$$\mu \geq \mu_0 = sF_{Max}/nF_{Max} \quad (4)$$

#### Design of orthogonal experiment

An orthogonal experiment was adopted to measure  $sF_{Max}$  and  $nF_{Max}$  and analyze the effect of sanding parameters on  $\mu$ . The parameters considered in the test were as follows: grit size ( $G$ ), feed speed ( $U$ ), sanding speed ( $V$ ), and sanding thickness ( $T_s$ ). Each factor had five levels (as shown in Table 1) with the (L25 ( $5^6$ )) orthogonal table. Each test was repeated three times under the same conditions to avoid any possible anomaly.

**Table 1.** Orthogonal Factors and Levels ( $G$ : grit size,  $U$ : feed speed,  $V$ : sanding speed,  $T_s$ : sanding thickness)

| Level | $G$ | $U$<br>(m/min) | $V$<br>(m/s) | $T_s$<br>(mm) |
|-------|-----|----------------|--------------|---------------|
| 1     | 40  | 2.52           | 5.35         | 0.1           |
| 2     | 60  | 3.00           | 6.69         | 0.2           |
| 3     | 80  | 3.72           | 8.04         | 0.3           |
| 4     | 100 | 4.44           | 9.38         | 0.4           |
| 5     | 120 | 5.16           | 10.74        | 0.5           |

Signal values of  $sF$  and  $nF$  generated by force sensor during the sanding process were captured by a signal collection device, and then transformed to the forces, as shown in Fig. 4. The  $sF$  measured in the test is the resultant force of sanding tangential force ( $sFt$ ) and radial force ( $sFr$ ) in the horizontal direction, and the  $nF$  is the resultant force of  $sFt$  and  $sFr$  in the vertical direction.

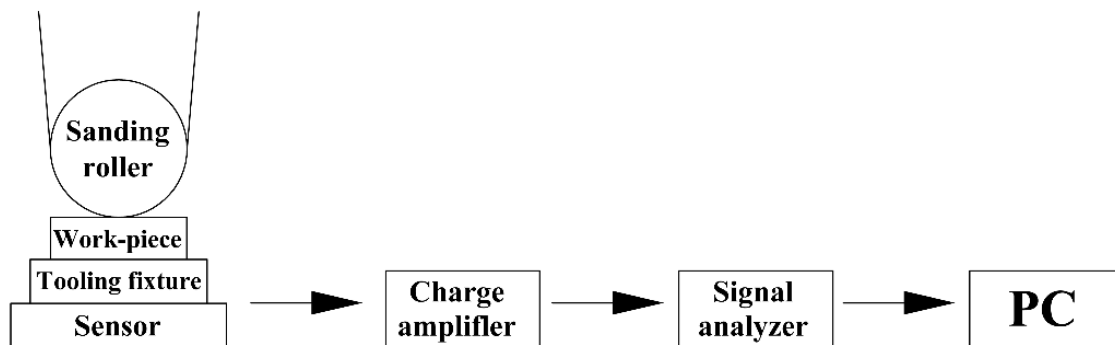


**Fig. 4.** Testing system of  $sF$  and  $nF$

## RESULTS AND DISCUSSION

### Relationships between $\mu$ and Intensity of Pressure ( $P$ ) for Six Types of Rubber Belts

Due to the elastic characteristics of rubber and wood based panel, values of  $\mu$  were variable under different test conditions. An exponential relationship was found between  $\mu$  and  $P$  for six types of rubber belt, and results are shown in Table 2.

**Table 2.** Relationships Between  $\mu$  and  $P$  ( $P$ : intensity of pressure ( $Pa$ ),  $\mu$ : static friction coefficient,  $MDF$ : medium density fiberboard,  $PB$ : particle board)

| Number of rubber belts | $MDF$                  | $R^2$  | $PB$                   | $R^2$  |
|------------------------|------------------------|--------|------------------------|--------|
| 1                      | $\mu=2.0769 P^{0.137}$ | 0.9386 | $\mu=1.9923 P^{0.125}$ | 0.9105 |
| 2                      | $\mu=2.4145 P^{0.199}$ | 0.9644 | $\mu=2.2971 P^{0.19}$  | 0.967  |
| 3                      | $\mu=3.201 P^{0.226}$  | 0.961  | $\mu=3.0893 P^{0.219}$ | 0.9661 |
| 4                      | $\mu=2.6471 P^{0.165}$ | 0.8635 | $\mu=2.4876 P^{0.155}$ | 0.8854 |
| 5                      | $\mu=2.0797 P^{0.19}$  | 0.9695 | $\mu=2.0766 P^{0.193}$ | 0.911  |
| 6                      | $\mu=2.8482 P^{0.201}$ | 0.9073 | $\mu=2.3453 P^{0.168}$ | 0.9339 |

### Calculating Results of $\mu_0$

During the sanding experiment, it was found that there was a linear relationship between  $sF_{Max}$  and  $nF_{Max}$  (according to the data of orthogonal experiment), so  $\mu_0$  was a constant. As shown in Figure 5, the  $\mu_0$  of  $MDF$  and  $PB$  were **0.7** and **0.712**, respectively.

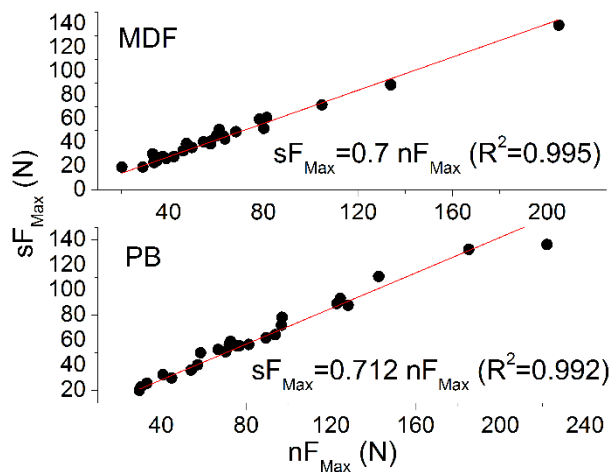


**Fig. 5.** Relationships between  $sF_{Max}$  and  $nF_{Max}$  in sanding process ( $sF_{Max}$ : maximum sanding force,  $nF_{Max}$ : maximum normal force)

### Analysis of $\mu$ During Sanding Process

The orthogonal experimental results of  $nF_{Max}$  and the  $P$  calculated by the corresponding values of  $nF_{Max}$  are shown in Table 3 (the contact area is  $0.0015 \text{ m}^2$ ,  $100 \text{ mm} \times 150 \text{ mm}$ , Eq. 2). Plugging the values of  $P$  into the equations in Table 2 to calculate  $\mu$  under the conditions of different sanding parameters, the results are shown in Table 4. The results indicate that only a few values of  $\mu$  overpassed the  $\mu_0$  values when using No.1

and No.4 rubber belts. This also means that the work-piece was relatively stationary only in a few situations when sanding with No. 1 and No. 4 rubber belts, and the average  $\mu$  values of both belts were higher than others. However, all of the average  $\mu$  values were lower than  $\mu_0$ , which means that a hold-down device or vacuum chuck should be equipped on the sanding machine for safety during operation.

**Table 3.** Orthogonal Experimental Results of  $nF_{Max}$  and the Corresponding  $P$  ( $nF_{Max}$ : maximal normal force,  $P$ : intensity of pressure,  $MDF$ : medium density fiberboard,  $PB$ : particle board)

| Test No. | MDF            |          | PB             |          |
|----------|----------------|----------|----------------|----------|
|          | $nF_{Max}$ (N) | $P$ (Pa) | $nF_{Max}$ (N) | $P$ (Pa) |
| 1        | 38.921         | 2594.76  | 29.620         | 1974.655 |
| 2        | 63.726         | 4248.37  | 54.058         | 3603.871 |
| 3        | 68.408         | 4560.51  | 72.103         | 4806.898 |
| 4        | 81.338         | 5422.56  | 96.713         | 6447.531 |
| 5        | 78.348         | 5223.20  | 122.879        | 8191.966 |
| 6        | 37.365         | 2491.03  | 70.343         | 4689.508 |
| 7        | 46.100         | 3073.35  | 66.884         | 4458.94  |
| 8        | 54.728         | 3648.51  | 72.665         | 4844.364 |
| 9        | 42.151         | 2810.09  | 33.156         | 2210.433 |
| 10       | 57.724         | 3848.24  | 57.166         | 3811.039 |
| 11       | 33.245         | 2216.31  | 58.517         | 3901.166 |
| 12       | 29.019         | 1934.58  | 30.341         | 2022.714 |
| 13       | 20.151         | 1343.41  | 40.723         | 2714.896 |
| 14       | 47.464         | 3164.25  | 96.930         | 6461.988 |
| 15       | 61.396         | 4093.10  | 142.626        | 9508.432 |
| 16       | 33.713         | 2247.54  | 44.790         | 2986.012 |
| 17       | 49.790         | 3319.35  | 89.357         | 5957.134 |
| 18       | 133.888        | 8925.90  | 222.059        | 14803.95 |
| 19       | 204.937        | 13662.49 | 185.142        | 12342.8  |
| 20       | 80.194         | 5346.27  | 81.229         | 5415.292 |
| 21       | 60.141         | 4009.39  | 76.831         | 5122.035 |
| 22       | 104.755        | 6983.64  | 124.493        | 8299.544 |
| 23       | 34.979         | 2331.95  | 75.280         | 5018.668 |
| 24       | 57.734         | 3848.91  | 93.730         | 6248.655 |
| 25       | 63.116         | 4207.74  | 128.169        | 8544.569 |

As for the inspection level,  $\alpha=0.01$ , the critical values can be found out from the distribution table of  $F$ :  $F_{0.01}(4, 8)=7.0$ , additionally, factors can be described as (\*) when  $F$  values overpass 7.0. Table 5 indicates that  $G$  had the greatest influence on  $\mu$  for both  $MDF$  and  $PB$ , but other sanding parameters' influences were not obvious.

Because  $G$  is the primary influence factor, a single-factor experiment was carried out to determine the relationship between  $G$  and  $\mu$ . The results are shown in Fig. 6. For both  $MDF$  and  $PB$ , similar with the orthogonal experimental results, when using No. 1 rubber belt,  $\mu$  was the greatest of all, and use of the No. 5 belt resulted in the smallest  $\mu$ . Additionally, a law can be found: the smaller the  $nF_{Max}$  was, the greater was  $\mu$  (for same rubber belt). For six types of rubber belt,  $\mu$  reached its peak when  $G$  equaled 80. On the contrary,  $nF_{Max}$  reached its nadir. The variation rates of  $\mu$  and  $nF_{Max}$  were coincident.

**Table 4.** Orthogonal Experimental Results of  $\mu$  (Bold type figure: overpass the critical static friction coefficient, *MDF*: medium density fiberboard, *PB*: particle board)

| Test No. | Number of rubber belts |      |      |             |      |      |             |      |      |             |      |      |
|----------|------------------------|------|------|-------------|------|------|-------------|------|------|-------------|------|------|
|          | <i>MDF</i>             |      |      |             |      |      | <i>PB</i>   |      |      |             |      |      |
|          | 1                      | 2    | 3    | 4           | 5    | 6    | 1           | 2    | 3    | 4           | 5    | 6    |
| 1        | <b>0.71</b>            | 0.51 | 0.54 | <b>0.72</b> | 0.47 | 0.59 | <b>0.77</b> | 0.54 | 0.59 | <b>0.77</b> | 0.48 | 0.66 |
| 2        | 0.66                   | 0.46 | 0.48 | 0.67        | 0.43 | 0.53 | <b>0.72</b> | 0.48 | 0.51 | 0.70        | 0.43 | 0.59 |
| 3        | 0.65                   | 0.45 | 0.48 | 0.66        | 0.42 | 0.52 | 0.69        | 0.46 | 0.48 | 0.67        | 0.40 | 0.56 |
| 4        | 0.64                   | 0.44 | 0.46 | 0.64        | 0.41 | 0.51 | 0.67        | 0.43 | 0.45 | 0.64        | 0.38 | 0.54 |
| 5        | 0.64                   | 0.44 | 0.46 | 0.64        | 0.41 | 0.51 | 0.65        | 0.41 | 0.43 | 0.62        | 0.36 | 0.52 |
| 6        | <b>0.71</b>            | 0.51 | 0.55 | <b>0.73</b> | 0.47 | 0.59 | 0.69        | 0.46 | 0.49 | 0.67        | 0.41 | 0.57 |
| 7        | 0.69                   | 0.49 | 0.52 | <b>0.70</b> | 0.45 | 0.57 | 0.70        | 0.47 | 0.49 | 0.68        | 0.41 | 0.57 |
| 8        | 0.68                   | 0.47 | 0.50 | 0.68        | 0.44 | 0.55 | 0.69        | 0.46 | 0.48 | 0.67        | 0.40 | 0.56 |
| 9        | 0.70                   | 0.50 | 0.53 | <b>0.71</b> | 0.46 | 0.58 | <b>0.76</b> | 0.53 | 0.57 | <b>0.75</b> | 0.47 | 0.64 |
| 10       | 0.67                   | 0.47 | 0.50 | 0.68        | 0.43 | 0.54 | <b>0.71</b> | 0.48 | 0.51 | 0.69        | 0.42 | 0.59 |
| 11       | <b>0.72</b>            | 0.52 | 0.56 | <b>0.74</b> | 0.48 | 0.61 | <b>0.71</b> | 0.48 | 0.51 | 0.69        | 0.42 | 0.58 |
| 12       | <b>0.74</b>            | 0.54 | 0.58 | <b>0.76</b> | 0.49 | 0.62 | <b>0.77</b> | 0.54 | 0.58 | <b>0.76</b> | 0.48 | 0.65 |
| 13       | <b>0.77</b>            | 0.58 | 0.63 | <b>0.81</b> | 0.53 | 0.67 | <b>0.74</b> | 0.51 | 0.55 | <b>0.73</b> | 0.45 | 0.62 |
| 14       | 0.69                   | 0.49 | 0.52 | <b>0.70</b> | 0.45 | 0.56 | 0.67        | 0.43 | 0.45 | 0.64        | 0.38 | 0.54 |
| 15       | 0.66                   | 0.46 | 0.49 | 0.67        | 0.43 | 0.54 | 0.63        | 0.40 | 0.42 | 0.60        | 0.35 | 0.50 |
| 16       | <b>0.72</b>            | 0.52 | 0.56 | <b>0.74</b> | 0.48 | 0.60 | <b>0.73</b> | 0.50 | 0.54 | <b>0.72</b> | 0.44 | 0.61 |
| 17       | 0.68                   | 0.48 | 0.51 | 0.69        | 0.45 | 0.56 | 0.67        | 0.44 | 0.46 | 0.65        | 0.39 | 0.54 |
| 18       | 0.60                   | 0.40 | 0.41 | 0.59        | 0.37 | 0.46 | 0.60        | 0.37 | 0.38 | 0.56        | 0.33 | 0.47 |
| 19       | 0.56                   | 0.36 | 0.37 | 0.55        | 0.34 | 0.42 | 0.61        | 0.38 | 0.39 | 0.58        | 0.34 | 0.48 |
| 20       | 0.64                   | 0.44 | 0.46 | 0.64        | 0.41 | 0.51 | 0.68        | 0.45 | 0.47 | 0.66        | 0.40 | 0.55 |
| 21       | 0.67                   | 0.46 | 0.49 | 0.67        | 0.43 | 0.54 | 0.68        | 0.45 | 0.48 | 0.66        | 0.40 | 0.56 |
| 22       | 0.62                   | 0.41 | 0.43 | 0.61        | 0.39 | 0.48 | 0.64        | 0.41 | 0.43 | 0.61        | 0.36 | 0.51 |
| 23       | <b>0.72</b>            | 0.52 | 0.55 | <b>0.74</b> | 0.48 | 0.60 | 0.69        | 0.46 | 0.48 | 0.66        | 0.40 | 0.56 |
| 24       | 0.67                   | 0.47 | 0.50 | 0.68        | 0.43 | 0.54 | 0.67        | 0.44 | 0.46 | 0.64        | 0.38 | 0.54 |
| 25       | 0.66                   | 0.46 | 0.49 | 0.67        | 0.43 | 0.53 | 0.64        | 0.41 | 0.43 | 0.61        | 0.36 | 0.51 |
| Avrg     | 0.68                   | 0.47 | 0.50 | 0.68        | 0.44 | 0.55 | 0.69        | 0.46 | 0.48 | 0.67        | 0.40 | 0.56 |

**Table 5.** Variance Analysis Table (*MDF*: medium density fiberboard, *PB*: particle board, *G*: grit size, *U*: feed speed, *V*: sanding speed, *T<sub>s</sub>*: sanding thickness)

| Factors   | <i>MDF</i>         |          | <i>PB</i>   |          |
|---|--------------------|----------|---|----------|
|   | Mean sum of square | <i>F</i> | Mean sum of square                                    | <i>F</i> |
| <i>G</i>  | 0.0183             | 8.83*    | 0.0107  | 8.13*    |
| <i>U</i>  | 0.0036             | 1.73     | 0.0008  | 0.64     |
| <i>V</i>  | 0.0034             | 1.65     | 0.0018  | 1.40     |
| <i>T<sub>s</sub></i>                                  | 0.0058             | 2.78     | 0.0028  | 2.15     |
| Error   | 0.0021             |          | 0.0013  |          |
| Orders of priorities of factors' influence            |                    |          |   |          |
| <i>G</i> > <i>T<sub>s</sub></i> > <i>U</i> > <i>V</i> |                    |          | <i>G</i> > <i>T<sub>s</sub></i> > <i>V</i> > <i>U</i> |          |

Increasing  $G$  partly results in the decreasing cutting force because of the increasing cutting edges in unit time (the removal of each cutting edge decrease). But with increasing  $G$ , the height of cutting edges becomes shorter, so greater pressure is required for normal cutting. Otherwise, the proportion of cutting force decreases and that of sanding friction increases (Graham and Abdullahi 1975). Meanwhile, the spaces between grits become smaller, for which it is difficult for the abrasive belt to discharge the sanding dust. So dust wraps the grits, then grits become blunt (blocked and blunting phenomenon), and finally the cutting force and sanding friction increase (Huang and Yang 2011). For  $sF_{Max}$  and  $nF_{Max}$ , they are not only the component forces of cutting, but also the component forces of sanding friction. So when sanding with different  $G$ , the final results of  $\mu$  depend on the proportions of cutting and friction.

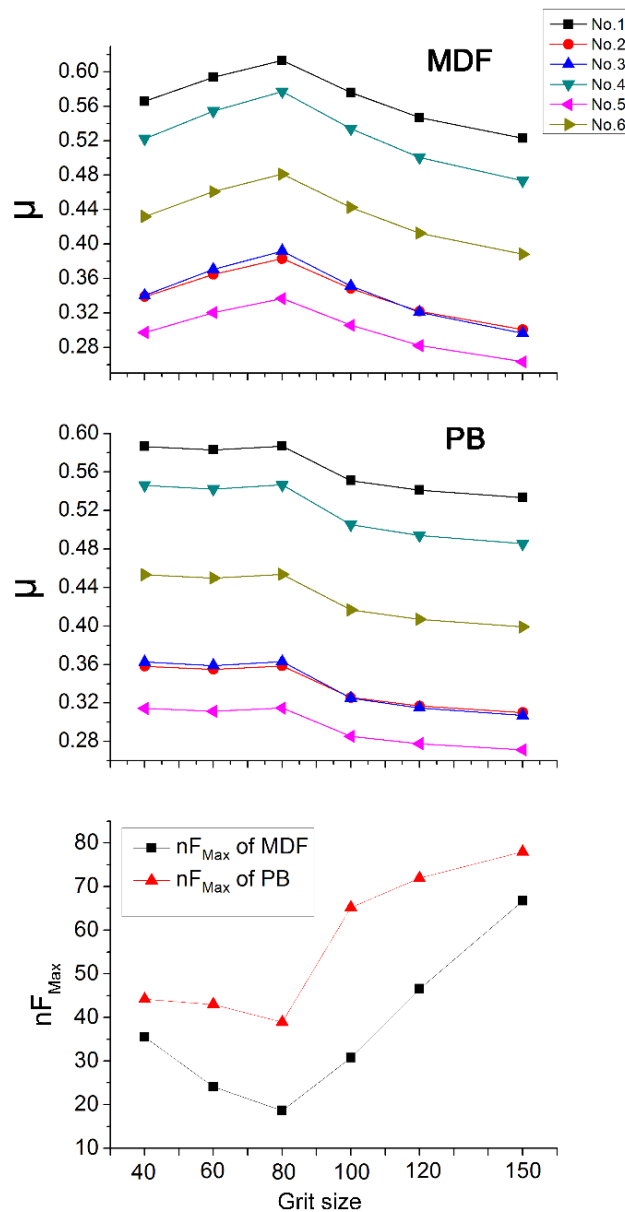


**Fig. 6.** Relationships between  $\mu$  and  $G$ ,  $nF_{Max}$  and  $G$  in sanding process (feed speed: 0.72 m/min, sanding speed: 8.04 m/s, sanding thickness: 0.5mm,  $\mu$ : static friction coefficient,  $nF_{Max}$ : maximum normal force, *MDF*: medium density fiberboard, *PB*: particle board)



### Analysis of $\mu$ of Different Rubber Belts

Due to the rough surface of a wood-based panel and the elastic characteristic of rubber, the distortional units of rubber filled into the gaps of work-piece surface, which resulted in an enlarged contact area between the rubber and work-piece, then the  $\mu$  and  $f$  increased (Fig. 7a). Thus, adopting softer rubber or increasing  $P$  on the work-piece can lead to the increasing value of  $f$  (for the same pattern of rubber belts). In other words, the level of elastic deformation increases (Wang and Yin 2009).

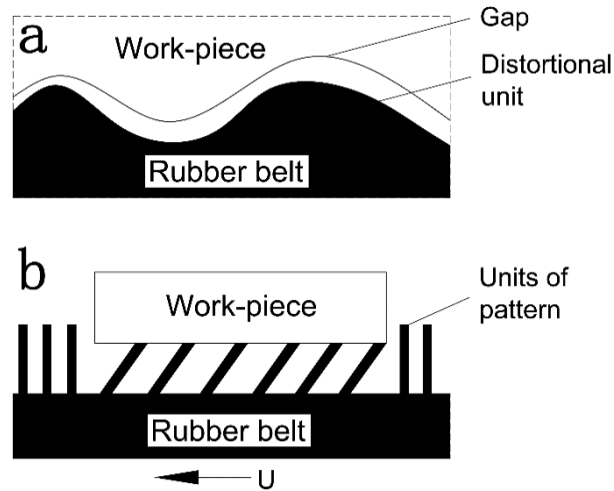


Fig. 7. Contact status between work-piece and rubber belt in sanding process

In this study, the surface hardness of all the rubber belts was the same, so different  $\mu$  values of rubber belts could be attributed to different patterns of the rubber belts. When No. 6 belt (without pattern) was used, the contact area between work-piece and rubber belt was the largest, which resulted in the lowest value of  $P$  and the fewest distortional units compared to the others. However, the average  $\mu$  of No. 6 was still greater than No. 2, No. 3, and No. 5 (Table 4 and Fig. 6). For belts of No. 2 and No. 5, the units of the patterns are independent, and tangential force on the contacted units cannot be shared by other non-contacted parts of the rubber belt (Fig. 1). So the units of pattern distort easily through the opposite direction of feeding, and if distortion overpasses elastic limit, the units of pattern may be fractured (Fig. 7b). In such a situation, the work-piece will move relative to the rubber belt, and  $\mu$  changes into dynamic friction coefficient ( $\mu_v$ ), thus  $f$  decreases.

### CONCLUSIONS

The critical static frictional coefficients ( $\mu_0$ ) and static frictional coefficients ( $\mu$ ) between work-piece and rubber belt during sanding *MDF* and *PB* were analyzed in this paper. The methods and results can provide some theoretical support for improving design techniques of sanding machine and choosing appropriate rubber belts for sanding wood based panel.

1. In this study,  $\mu_0$  is a constant that can be calculated by  $sF_{Max}$  and  $nF_{Max}$ . Besides, there is an exponential relationship between  $P$  and  $\mu$ .

2. For both *MDF* and *PB*, *G* has the greatest impact on  $\mu$  among all sanding parameters. In the single-factor experiment, for six types of rubber belts, when *G* equals to 80,  $\mu$  reaches its peak, and the smaller the  $nF_{Max}$  is, the greater the  $\mu$  is (for same rubber belts), but the variation rates of  $\mu$  and  $nF_{Max}$  are coincident.

3. The average  $\mu$  of No. 1 and No. 4 are greater than others, but average  $\mu$  of all the rubber belts are lower than  $\mu_0$ . So when adopting such six types of rubber belts, a hold-down device or vacuum chuck should be equipped on the sanding machine.

4. Patterns of rubber belts have some impact on  $\mu$ , and appropriate patterns on the surface of rubber belts contribute to higher  $\mu$ .

## ACKNOWLEDGMENTS

This paper was financially supported by the Special Fund for Forestry Research in the Public Interest (Project 201204703-B2)

## REFERENCES CITED

- Guan, N., Thunell, B., and Lyth, K. (1983). "On the friction between steel and some common Swedish wood species," *Eur. J. Wood Wood Prod.* 41, 55-60. DOI: 10.1007/BF02612232
- Graham, W., and Abdullahi, A. T. (1975). "The nature of wheel-work piece contact in surface grinding," *International Journal of Machine Tool Design and Research* 15(3), 153-160.
- Han, L., Zhang, D. W., and Wang, F. J. (2013). "Predicting film parameter and friction coefficient for helical gears considering surface roughness and load variation," *Tribology Transactions* 56(1), 49-57. DOI:10.1080/10402004.2012.725806
- Huang, Y., and Yang, C. Q. (2011). "Experimental research on abrasive belt grinding for 304 stainless steel," *China Mechanical Engineering* 22(3), 291-295.
- Jun, X. (2008). "Rubber friction," *World Rubber Industry* 35(12), 42.
- Li, L., and Meng, J. J. (2000). "Analysis of feeding force on sanding wood piece and the safety measures," *China Wood Industry* 14(3), 36-37.
- Masuko, M., Aoki, S., and Suzuki, A. (2005). "Influence of lubricant additive and surface texture on the sliding friction characteristics of steel under varying speeds ranging from ultralow to moderate," *Tribology Transactions* 48(3), 289-298. DOI:10.1080/05698190590965558
- Wang, B. S., and Yin, Y. Y. (2009). "Study on the tribological properties between rubber and floor tile," *Materials Review* 23(9), 113-117.

Article submitted: August 22, 2014; Peer review completed: September 27, 2014;  
Revised version received and accepted: October 19, 2014; Published: October 23, 2014.